Volume 47
Number 15
21 April 2023
Pages 6997–7448

NJC

New Journal of Chemistry

A journal for new directions in chemistry

rsc.li/njc

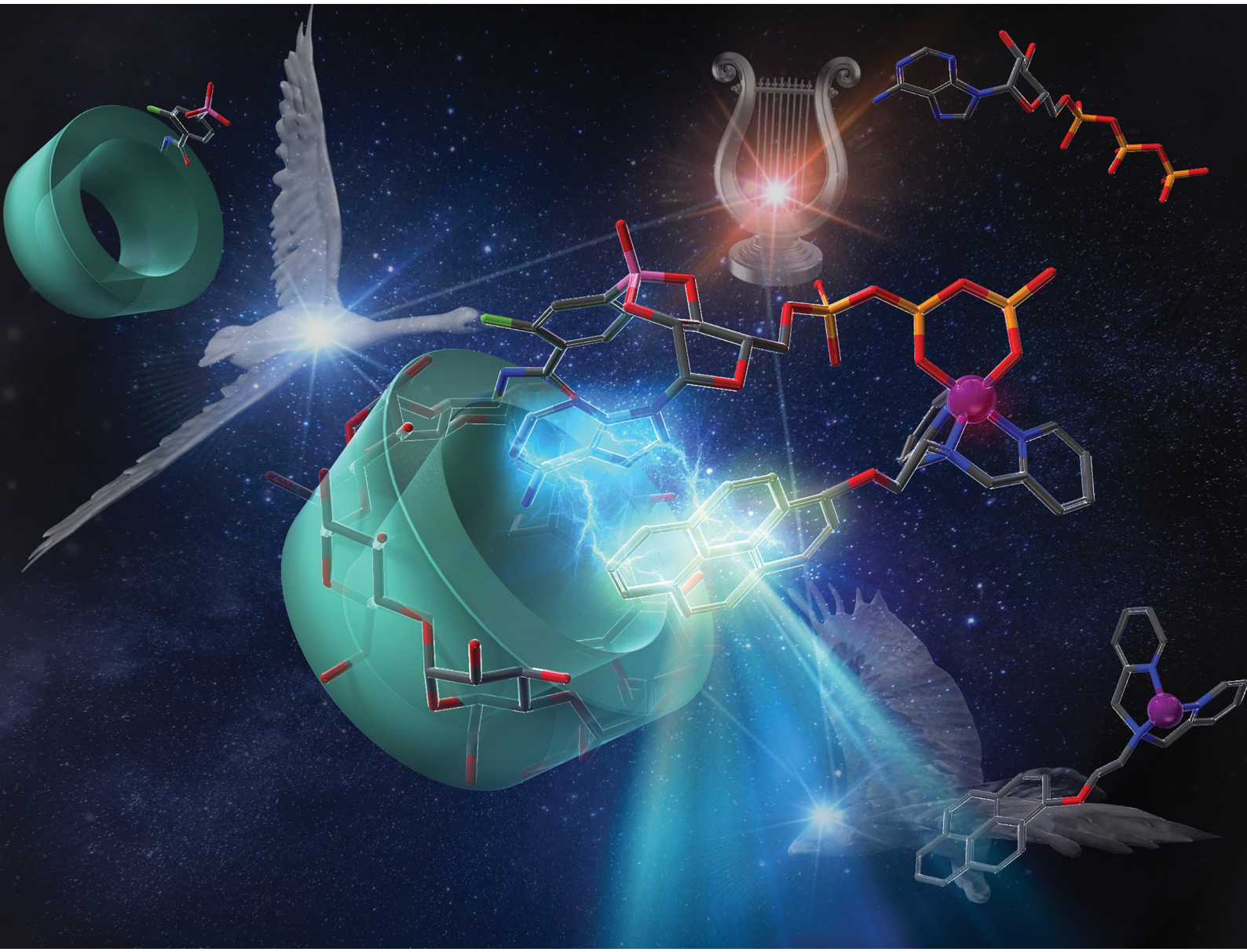

ISSN 1144-0546

ROYAL SOCIETY OF CHEMISTRY

PAPER

Takashi Hayashita *et al.*

Selective ATP recognition by boronic acid-appended cyclodextrin and a fluorescent probe supramolecular complex in water

cnrs

NJC

ROYAL SOCIETY OF CHEMISTRY

PAPER

View Article Online
View Journal | View Issue

Cite this: *New J. Chem.*, 2023, **47**, 7035

Selective ATP recognition by boronic acid-appended cyclodextrin and a fluorescent probe supramolecular complex in water†

Yota Suzuki, ‡ Masakage Masuko,‡ Takeshi Hashimoto and Takashi Hayashita *

Received 10th January 2023,
Accepted 23rd February 2023

DOI: 10.1039/d3nj00139c

rsc.li/njc

Various organic compound-based chemosensors for adenosine triphosphate (ATP) have been reported; however, the conventional designs have problems with their water solubility, selectivity, and sensitivity. Herein, a supramolecular complex of boronic acid-appended γ-cyclodextrin and zinc-dipicolylamine-based pyrene probe (**Zn-1/FBγCyD**) was designed based on the concept of a "cyclodextrin (**CyD**)-based supramolecular chemosensor". As a proof-of-concept, we have demonstrated that this complex exhibits a turn-on fluorescence response to ATP in water at physiological pH with excellent selectivity and sensitivity, owing to the efficient self-assembly of **Zn-1/FBγCyD** with ATP through synergistic interactions to afford a strongly fluorescent product. Remarkably, **Zn-1/FBγCyD** demonstrated extremely strong affinity for ATP with the conditional formation constant of $(7.71 \pm 0.09) \times 10^6$ M^{-1}, resulting in the low limit of detection of 18.9 nM. Furthermore, **Zn-1/FBγCyD** can monitor changes in ATP concentration after the addition of apyrase, hydrolysing ATP to adenosine monophosphate and a phosphate ion. We believe that the presented approach of a **CyD**-based supramolecular chemosensor will propose a novel design that realises unexplored selectivity in the research field of fluorescent molecular recognition.

Introduction

The field of fluorescence recognition for application to the fluorometric sensing of biologically important analytes has advanced tremendously.[1,2] In particular, chemosensors for adenosine triphosphate (ATP) have attracted significant attention given the various important roles that ATP plays in biological processes as the energy currency of cells;[3] for example, metabolism,[4] cellular signalling,[5] and protein synthesis.[6] The chemosensing approach for the detection of ATP has several advantages, including ease of use, low cost, and high accuracy, overcoming the drawbacks of the conventional luciferin–luciferase assay for ATP sensing, which has low stability and accuracy and requires cumbersome operations.[7,8]

The strategic design of ATP-selective chemosensors is mainly based on multitopic receptors that capture several recognisable moieties of ATP, namely, the ribose, triphosphate, and adenine units.[3,9,10] Despite extensive developments in this research area, most previously designed chemosensors are based on organic scaffolds and are sometimes poorly soluble in water requiring 10 vol% or more organic solvent.[11–14] Moreover, designing highly selective ATP chemosensors has been challenging because of structural similarities among phosphate derivatives including polyphosphates and nucleotides.[15,16] Selectivity is an important issue for applications in biological research; for example, chemosensors that allow for the discrimination of ATP from adenosine diphosphate (ADP), adenosine monophosphate (AMP), and the pyrophosphate ion (PPi) are useful in gaining a better understanding of cellular processes.[17,18] However, conventional strategies require careful organic synthesis and given the difficulty in attaining high selectivity for ATP, reports of ideal chemosensors that exhibit a turn-on response to only ATP have been scarce.

We previously presented a concept of multidentate recognition by water-soluble supramolecular chemosensors based on binding unit-appended cyclodextrins (**CyDs**) with fluorescent and colorimetric probes.[19–22] As the assembly behaviour of **CyD** is highly sensitive to the structures of the components, the **CyD**-based supramolecular chemosensors display a variety of responses depending on the analyte structure: this feature is advantageous because it provides excellent selectivity for the target analyte (Fig. 1a). Based on these previous studies, we report

Department of Materials and Life Sciences, Faculty of Science and Technology, Sophia University, 7-1, Kioi-cho, Chiyoda-ku, Tokyo, 102-8554, Japan
E-mail: ta-hayas@sophia.ac.jp

† Electronic supplementary information (ESI) available: Experimental details, synthetic procedures, Fig. S1–S32, Charts S1–S3, and Scheme S1. See DOI: https://doi.org/10.1039/d3nj00139c

‡ These authors contributed equally.

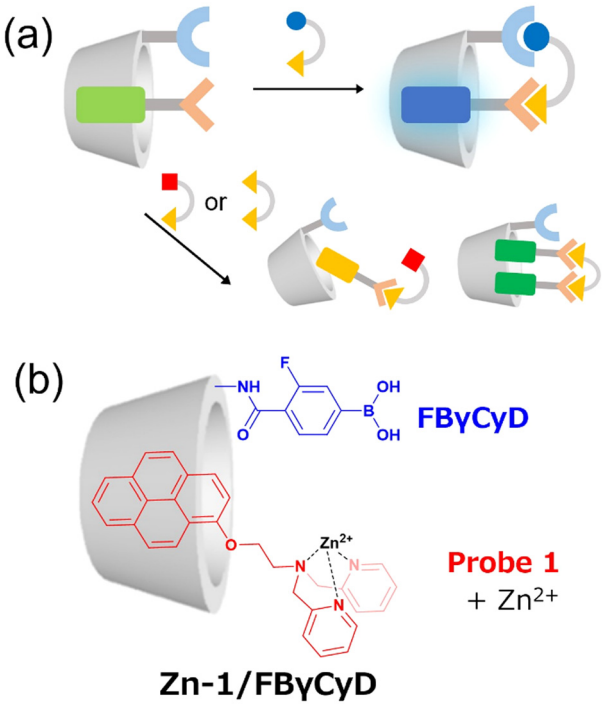

Fig. 1 (a) Cartoon representation of the concept of **CyD**-based supramolecular chemosensors based on a modified CyD with fluorescent probes. (b) Structure of **Zn-1/FBγCyD**.

a supramolecular complex (**Zn-1/FBγCyD**) of fluorophenylboronic acid-appended γCyD (**FBγCyD**) and a Zn(II)-dipicolylamine (**Zn-dpa**)-based fluorescent probe (**Zn-1**) as a proof-of-concept to design a multitopic **CyD**-based supramolecular chemosensor for ATP showing turn-on fluorescence response (Fig. 1b). **FBγCyD** has one fluorophenylboronic acid moiety introduced at the C3 position of one 1,4-glycopyranoside unit on the secondary rim. The boronic acid and **Zn-dpa** moieties capture the ribose and triphosphate units of ATP, respectively.[11,17] The electron-withdrawing fluorine group is introduced to increase the Lewis acidity of the boron centre; boronic acids with high acidity react with 1,2-diol compounds efficiently.[23] The **Zn-1/FBγCyD** complex displays specific fluorescence enhancement in response to only ATP.

Experimental

Reagents

All reagents were purchased from commercial sources and used as received without further purification. The detailed information is summarised in the ESI.†

Instruments

All the nuclear magnetic resonance (NMR) spectra were measured by using a JEOL JNM-ECA 500 spectrometer (JEOL, Japan) at room temperature. For ^{1}H and ^{13}C NMR spectroscopy, the solvent signals were used as ref. 24 The high resolution electrospray ionization mass spectra (HRMS-ESI) were recorded in methanol using a JEOL Accu-TOF JMS T100LC (JEOL, Japan). The high resolution fast atom bombardment mass spectra (HRMS-FAB) were recorded using a MStation JMS-700 (JEOL, Japan). Solution pH was measured by using a HORIBA pH meter F-52 (Horiba, Japan). The UV-vis absorption spectra were measured using a Hitachi U-3900H absorption spectrophotometer (Hitachi, Japan) equipped with a temperature controller (Hitachi, Japan) to keep the temperature constant at 25 °C. The fluorescence spectra were measured using a Hitachi F-7000 fluorescence spectrophotometer (Hitachi, Japan) and a Hitachi F-7100 fluorescence spectrophotometer (Hitachi, Japan) equipped with a temperature controller (Hitachi, Japan) and an EYELA CCA-1111 (EYELA, Japan) to keep the temperature constant at 25 °C. The induced circular dichroism (ICD) spectra were measured using a JASCO J-820 spectrophotometer (JASCO, Japan) equipped with a Peltier temperature controller (JASCO, Japan) and an EYELA Cool Ace CA-1111 (EYELA, Japan) to keep the temperature constant at 25 °C under a nitrogen atmosphere.

Preparation of sample solutions

All sample solutions were prepared with Milli-Q water and spectroscopic-grade dimethyl sulfoxide (DMSO) using acid-washed glassware. Unless otherwise noted, a mixed solvent system of DMSO/water (1/99 in v/v) was used. The pH of the solutions for spectroscopic measurements was adjusted to 7.4 with diluted aq. HCl and aq. NaOH in the presence of 5 mM 4-(2-hydroxyethyl)-1-piperazineethanesulfonic acid (HEPES) buffer. Appropriate amounts of DMSO and the following stock solutions: probe **1** DMSO solution (10 mM), an aq. zinc(II) ion (4 mM), aq. **FBγCyD** (5 mM), a pH buffer solution (50 mM), and an aq. phosphate derivative, were added into a volumetric flask to adjust the concentrations for each experimental condition. Basically, the sample solutions contain 10 μM of **1**, 10 μM of Zn^{2+}, 0.1 or 0.5 mM of **FBγCyD**, and 5 mM of HEPES in DMSO/water (1/99 in v/v). Before the measurements of the fluorescence and UV-vis absorption spectra, all the sample solutions were vortexed for 10 seconds.

Determination of acid dissociation constant

The absorbance of **FBγCyD** at a specific wavelength was measured and analysed using the KaleidaGraph program based on the acid dissociation model of monobasic acids.

Determination of inclusion constants

Fluorescence intensity changes ($F - F_0$) of **Zn-1** at various concentrations of cyclodextrin compounds were analysed using KaleidaGraph program to determine the inclusion constants.

Determination of conditional equilibrium constants

Multi-wavelength data (360–600 nm) of the fluorescence spectra at various concentrations of phosphate derivatives were analysed using the ReactLab EQUILIBRIA program to determine the conditional equilibrium constants.[25]

Monitoring of the change in ATP concentrations

Fluorescence intensity changes at 386 nm were monitored for 1200 seconds with stirring using an Hitachi F-7100 fluorescence spectrophotometer after the apyrase addition (100 mU,

50 mU, and 10 mU) into **Zn-1/FBγCyD-ATP** solution. During these measurements, the temperature was kept constant at 25 °C.

Results and discussion

Probe **1** and modified **CyD**s were readily synthesised (see ESI† and Fig. S1–S4). **Zn-1** was prepared by the addition of zinc nitrate (10 μM) to an equimolar amount of **1** (C_1 = 10 μM) in a mixed solvent of DMSO and water (1/99 in vol.). The acid dissociation constant (pK_a) of the boronic acid moiety was determined to be 7.92 ± 0.02 from the pH-dependence of the UV-vis absorption spectra of **FBγCyD** (Fig. S5 and S6, ESI†), indicating that 23% of **FBγCyD** is present as the conjugate tetrahedral boronate anion at pH 7.4 (Scheme S1, ESI†).[23]

The fluorescence intensity of **Zn-1** was enhanced by increasing the concentration of coexisting **FBγCyD** (Fig. S7, ESI†), suggesting that the supramolecular encapsulation of **Zn-1** by **FBγCyD** suppresses the non-radiative decay of the excited state.[26] Although the **γCyD** cavity forms a pyrene dimer that exhibits dimeric fluorescence at approximately 500 nm,[27] this was not observed for the supramolecular complex of **FBγCyD** with **Zn-1**. This finding suggests that **FBγCyD** and **Zn-1** form a supramolecular complex in a 1 : 1 stoichiometric ratio, *i.e.*, **Zn-1/FBγCyD**. The changes in the fluorescence intensity of **Zn-1** at various **FBγCyD** concentrations were well fitted to the 1 : 1 stoichiometric inclusion model, with an inclusion constant of (3.08 ± 0.08) × 10^5 M^{-1} (Fig. S7, ESI†). In contrast, the fluorescence enhancement observed with the addition of **FBγCyD** was not apparent when native **γCyD** was added to **Zn-1** (Fig. S8, ESI†); the inclusion constant was much smaller at (4.25 ± 0.73) × 10^3 M^{-1} (Fig. S9, ESI†). These findings suggest that the incorporated boronic acid moiety of **FBγCyD** facilitates the tight supramolecular complexation of **Zn-1/FBγCyD** *via* electrostatic attraction between the positive **Zn-dpa** moiety of **Zn-1** and the negative boronate species of **FBγCyD** partially present in the solution.

To determine the selectivity of **Zn-1/FBγCyD** for ATP, the UV-vis absorption and fluorescence spectra of **Zn-1/FBγCyD** were measured in the absence and presence of various phosphate derivatives: phosphate ion (Pi), PPi, triphosphate ion (Tri), AMP, ADP, and ATP (Chart S1, ESI†). Whereas no differences in the UV-vis absorption spectra were observed (Fig. S10, ESI†), the fluorescence spectra varied depending on the added phosphate derivatives (Fig. 2). In the absence of the phosphate derivatives, **Zn-1/FBγCyD** exhibited a vibronic-structured fluorescence band in the 370 to 450 nm region, which is a characteristic spectral pattern of pyrene compounds.[28] The addition of the inorganic polyphosphates (PPi and Tri) resulted in a clear reduction in fluorescence intensity. The PPi moiety efficiently coordinates to the Zn(II) centres of two **Zn-dpa** moieties to form a bis-dentate complex, *i.e.*, PPi-bis[**Zn-dpa**].[15] As shown in the normalised spectra of Fig. 2a, the dimeric fluorescence of the pyrene moieties was clearly observed at approximately 500 nm in the presence of PPi and Tri (Fig. S11, ESI†). Thus, the decrease in fluorescence is attributable to the

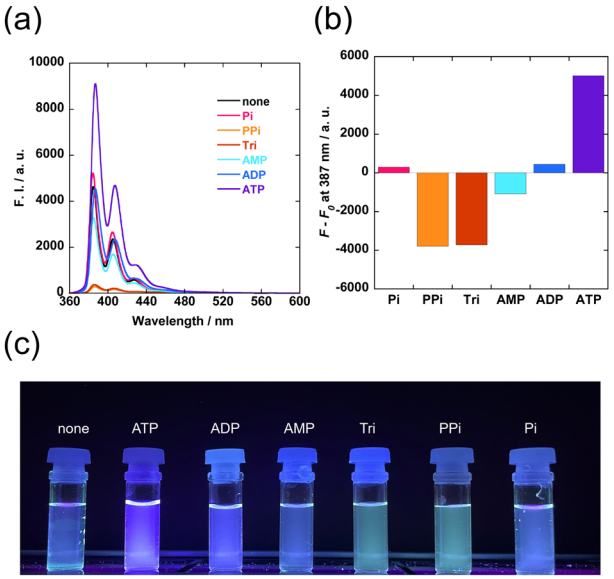

Fig. 2 The fluorescence spectra of **Zn-1/FBγCyD** (a) and fluorescence enhancement ($F - F_0$) at 387 nm of **Zn-1/FBγCyD** (b) in the absence and presence of various 1.0 mM phosphate derivatives in DMSO/water (1/99 in vol.): C_1 = 10 μM, C_{Zn} = 10 μM, $C_{\mathbf{FB\gamma CyD}}$ = 0.5 mM, C_{HEPES} = 5 mM, pH 7.4, T = 25 °C, and λ_{ex} = 350 nm. Photographs of sample solutions with 365 nm UV irradiation at room temperature (c).

formation of the inclusion complex of the **Zn-1** dimer with **FBγCyD** and the inorganic polyphosphates, **PPi-** and **Tri-(Zn-1)$_2$/FBγCyD** (Chart S2, ESI†), which quenches the monomeric fluorescence. Pi, AMP, and ADP caused almost no changes in the fluorescence spectra of **Zn-1/FBγCyD**, suggesting that these phosphate derivatives inefficiently react with **Zn-1/FBγCyD**. Surprisingly, **Zn-1/FBγCyD** exhibited a fluorescence turn-on response to only ATP, demonstrating its excellent selectivity for ATP: this supramolecular complex can discriminate between ATP and other typical interfering phosphate derivatives, such as PPi and ADP, which give indistinguishable fluorescence spectra in many reported systems.[15] Notably, the change in fluorescence colour was visible to the naked eye (Fig. 2c).

The fluorescence spectra of **Zn-1/FBγCyD** were measured at various concentrations of the phosphate derivatives (Fig. 3 and Fig. S12–S17, ESI†). As shown in Fig. 2, the fluorescence enhancement of **Zn-1/FBγCyD** was observed only with the addition of ATP. The change in fluorescence intensity reached saturation when the total concentration of ATP was 10 μM (the same as **Zn-1** concentration): this result signifies that **Zn-1/FBγCyD** quantitatively reacts with ATP. The conditional equilibrium constant was determined to be (7.71 ± 0.09) × 10^6 M^{-1} according to the 1 : 1 binding model (Fig. S18, ESI†). The extremely large affinity gave rise to the excellent sensitivity to ATP, with a low limit of detection of 18.9 nM (Fig. S19, ESI†). For PPi and Tri, spectral changes were well fitted to the 2 : 1 binding model (probe: phosphate), supporting that **Zn-1** forms dimers with PPi and Tri inside the **FBγCyD** cavity (Fig. S20 and S21, ESI†).

As competitive experiments, the fluorescence spectra of **Zn-1/FBγCyD** with ATP (**Zn-1/FBγCyD-ATP**) were measured in

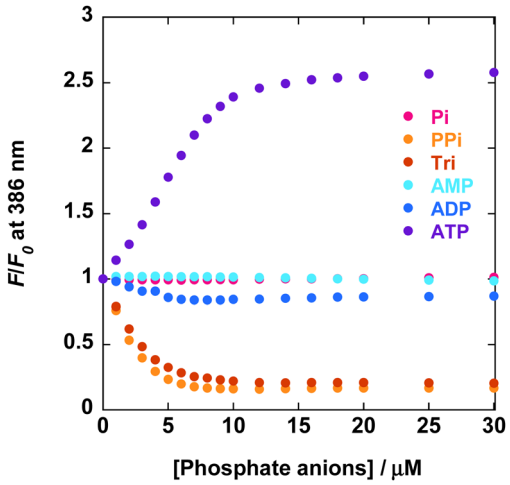

Fig. 3 Fluorescence intensity ratios (F/F_0) at 386 nm of **Zn-1/FBγCyD** at various phosphate concentrations in DMSO/water (1/99 in vol.): C_1 = 10 μM, C_{Zn} = 10 μM, $C_{\mathbf{FB\gamma CyD}}$ = 0.1 mM, C_{HEPES} = 5 mM, pH 7.4, T = 25 °C, and λ_{ex} = 350 nm.

the presence of the other phosphate derivatives as competitors (Fig. S22, ESI†). The fluorescence intensity of **Zn-1/FBγCyD-ATP** remained unchanged by the addition of AMP and ADP, demonstrating the high selectivity of the complex for ATP even in the presence of other adenine nucleotides. Although the additions of PPi and Tri decreased the fluorescence intensity of **Zn-1/FBγCyD-ATP**, the turn-on response of **Zn-1/FBγCyD** to ATP was partially preserved. Given that ATP is present in large amounts among phosphate derivatives in both intracellular and extracellular environments,[29] the presence of competitors should not significantly affect the sensitivity to ATP. Taken together, **Zn-1/FBγCyD** is potentially useful in practical situations where ATP measurement is performed in the presence of other phosphate derivatives.

To clarify the role of the boronic acid moiety of **FBγCyD**, the fluorescence spectra of **Zn-1** with phosphate derivatives were measured in the absence of **FBγCyD** (Fig. S23, ESI†) and the presence of native **γCyD** (Fig. S24, ESI†) and phenyl-appended **γCyD** (**PhγCyD**, Fig. S25, ESI†). In all the systems, fluorescence enhancement was observed in response to all phosphate derivatives except Pi, suggesting that **Zn-1/γCyD**, **Zn-1/PhγCyD**, or **Zn-1** alone shows no sensitivity to ATP. The observed fluorescence enhancement is likely due to the suppression of the photo-induced electron transfer quenching process by the complexation of the **Zn-dpa** moiety with the phosphate moieties, which decreases the cationic character of the zinc centre.[15] These results clearly show that the boronic acid moiety incorporated into **FBγCyD** plays an essential role in improving the selectivity for ATP, plausibly due to the binding of the boronic acid moiety to the 1,2-diol moiety of ATP. Therefore, the observed ATP selectivity of **Zn-1/FBγCyD** is surely originated from the multiple bindings with ATP. In other words, **Zn-1/FBγCyD** possesses binding sites that are structurally unsuitable for the multidentate recognition of AMP and ADP, and **FBγCyD** facilitates the formation of **PPi-** and **Tri-(Zn-1)$_2$/FBγCyD** with PPi and Tri, respectively, which results in the quenching of the monomer fluorescence. Such dimer formation does not occur in the **Zn-1/γCyD** and **Zn-1/PhγCyD** systems because **γCyD** and **PhγCyD** do not tightly encapsulate **Zn-1**. As mentioned, multidentate recognition by the **Zn-dpa** moiety and the boronic acid moiety of **Zn-1/FBγCyD** was suggested in binding to **ATP**. As controls, the fluorescence spectra of **Zn-1/γCyD** and **Zn-1/PhγCyD** were measured in the presence of ATP (Fig. S26, ESI†). Both supramolecular complexes showed much weaker fluorescence than **Zn-1/FBγCyD-ATP**. This suggests that the boronic acid moiety rigidifies the pyrene fluorophore through multidentate recognition and therefore supports the expected multidentate recognition.

The supramolecular complex structures of **CyD** with a pyrene compound vary depending on the ring size of **CyD**; pyrene compounds form 2 : 1 and 1 : 1 (pyrene:**CyD**) stoichiometric supramolecular complexes with **γCyD** and **βCyD**, respectively.[27] Therefore, the effect of **CyD** ring size on selectivity was also investigated by using native **βCyD** and fluorophenylboronic acid-appended **βCyD** (**FBβCyD**) instead of **FBγCyD** (Chart S3, ESI†). The corresponding **βCyD**-based supramolecular complexes, *i.e.*, **Zn-1/βCyD** (Fig. S27, ESI†) and **Zn-1/FBβCyD** (Fig. S28, ESI†), showed similar trends with **Zn-1** alone, **Zn-1/γCyD**, and **Zn-1/PhγCyD**, exhibiting fluorescence enhancement in response to all phosphate derivatives except Pi. This finding indicates that the signaling mechanisms of **Zn-1/βCyD** and **Zn-1/FBβCyD** are essentially the same as **Zn-1** alone, **Zn-1/γCyD**, and **Zn-1/PhγCyD**, clearly signifying that the **FBγCyD** host provides overwhelmingly superior ATP selectivity compared with other **CyD** hosts.

The induced circular dichroism (ICD) spectra of **Zn-1/FBγCyD** were measured in the absence and presence of phosphate derivatives to further extract structural information (Fig. S29, ESI†). The supramolecular complexation of **FBγCyD** with **Zn-1** led to a strongly positive Cotton effect at 350 nm. This result empirically demonstrates that **Zn-1** is encapsulated by the cavity of **FBγCyD**.[30] When the phosphate derivatives having pyrophosphate moieties (PPi, Tri, and ATP) were present, the intensity of ellipticity at 350 nm was markedly decreased. This implies that the pyrophosphate moieties coordinate to the **Zn-dpa** moiety of **Zn-1/FBγCyD**.

The selectivity of **Zn-1/FBγCyD** for ATP was further examined by screening other nucleotides (Chart S1, ESI†) including guanosine triphosphate (GTP), cytidine triphosphate (CTP), and uridine triphosphate (UTP). The additions of CTP and UTP attenuated the fluorescence intensity, whereas the addition of GTP enhanced the fluorescence intensity (Fig. 4). These results suggest that the purine bases play a vital role in triggering the turn-on response of **Zn-1/FBγCyD**. The adenine moiety of ATP may form π–π stacking with the pyrene moiety of the **Zn-1** unit in the **CyD** cavity to further rigidify the **Zn-1** unit, given that **CyD** cavities encapsulate the adenine moiety in water.[31,32] As **Zn-1/FBγCyD-ATP** emits stronger fluorescence than **Zn-1/FBγCyD-GTP**, the assembly with ATP is expected to be more efficient than with GTP.

The obtained results indicate that **Zn-1** and **FBγCyD** form a rigid supramolecular complex that features three-point recognition

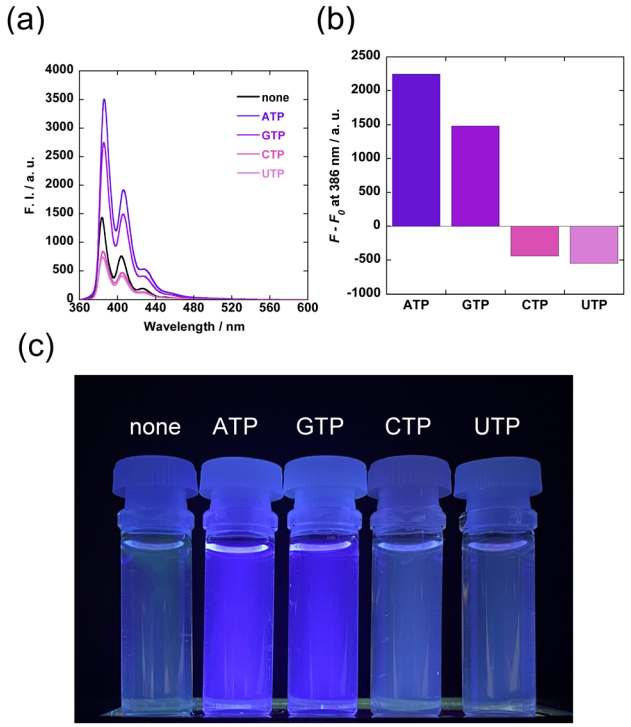

Fig. 4 The fluorescence spectra of **Zn-1/FBγCyD** (a) and changes in the fluorescence intensity ($F - F_0$) at 386 nm of **Zn-1/FBγCyD** (b) in the absence and presence of 1 mM of various nucleotides in DMSO/water (1/99 in vol.): C_1 = 10 μM, C_{Zn} = 10 μM, $C_{\mathbf{FB\gamma CyD}}$ = 0.1 mM, C_{HEPES} = 5 mM, pH 7.4, T = 25 °C, and λ_{ex} = 350 nm. Photographs of the sample solutions with 365 nm UV irradiation at room temperature (c).

including (1) esterification of the boronic acid and ribose moieties, (2) complexation of the **Zn-dpa** and triphosphate moieties, and (3) π–π stacking between the pyrene and adenine moieties (Fig. 5). On the contrary, the additions of PPi and Tri result in fluorescence reduction, as the formation of the **Zn-1** dimer leads to quenching of the monomeric fluorescence. For the recognition of AMP and ADP, the binding sites of **Zn-1/FBγCyD** are structurally mismatched; hence, the excellent selectivity for ATP is due to the various responses of the **CyD**-based supramolecular chemosensor to different analyte structures.

Zn-1/FBγCyD was evaluated for potential application to the monitoring of ATP concentrations. Apyrase was added to a solution containing **Zn-1/FBγCyD** and ATP (30 μM) in order to hydrolyse ATP *via* conversion into ADP and AMP, as follows: (1) ATP → ADP + Pi, and (2) ADP → AMP + Pi.[33] Changes in fluorescence intensity at 386 nm were monitored during this hydrolysis reaction (Fig. 6). **Zn-1/FBγCyD** was robust to apyrase under these experimental conditions (Fig. S30, ESI†). After the addition of apyrase, the fluorescence intensity of **Zn-1/FBγCyD-ATP** at 386 nm gradually decreased with time. The rate of hydrolysis of ATP increased with increasing apyrase concentration; this clearly shows that ATP is hydrolysed by apyrase. After the hydrolysis reaction was completed, the fluorescence of **Zn-1/FBγCyD** was recovered (Fig. S31 and S32, ESI†). These results suggest that ATP is completely hydrolysed to AMP and Pi without any influence on the **Zn-1/FBγCyD** fluorescence spectra

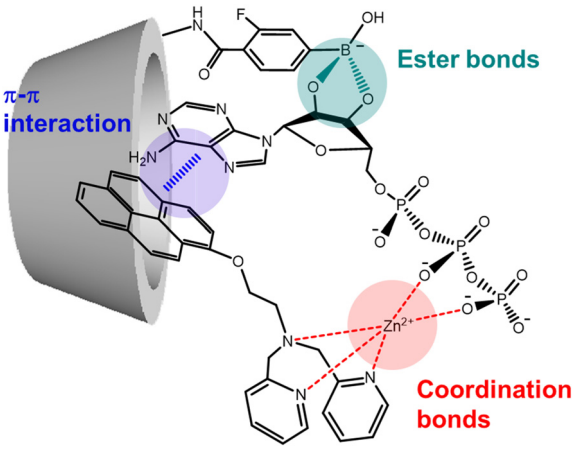

Fig. 5 Plausible structure of **Zn-1/FBγCyD-ATP**.

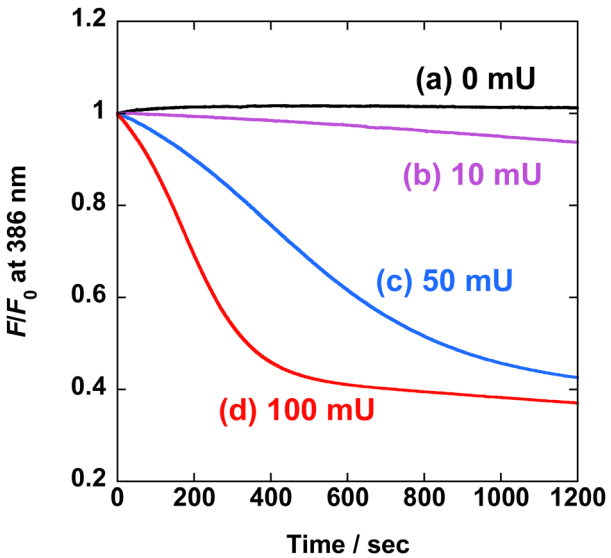

Fig. 6 Changes in relative fluorescence intensity (F/F_0) at 386 nm of **Zn-1/FBγCyD** with ATP (30 μM) in DMSO/water (1/99 in vol.) following the addition of apyrase: (a) 0 mU, (b) 10 mU, (c) 50 mU, and (d) 100 mU: C_1 = 10 μM, C_{Zn} = 10 μM, $C_{\mathbf{FB\gamma CyD}}$ = 0.1 mM, C_{HEPES} = 5 mM, pH 7.4, T = 25 °C, and λ_{ex} = 350 nm.

(Fig. 2). Consequently, **Zn-1/FBγCyD** allows for the monitoring of changes in ATP concentration with time. This feature is potentially advantageous when applied to biological studies to examine cellular processes relating to ATP production and consumption.

Conclusions

We have designed a **CyD**-based supramolecular chemosensor, **Zn-1/FBγCyD**, which selectively recognises ATP and allows for the monitoring of changes in ATP concentration with time. Its excellent selectivity is due to the efficient assembly of **Zn-1/FBγCyD** with ATP, which is facilitated by synergistic multi-recognition to form a fluorescent supramolecular product.

Surprisingly, **Zn-1/FBγCyD** demonstrated extremely strong affinity for ATP, achieving the detection of ATP with nM levels. In other words, we have demonstrated that the concept of a **CyD**-based supramolecular chemosensor has benefits providing various advantageous features compared to simple fluorescent probes, such as water solubility, excellent selectivity, and sensitivity. We believe that **Zn-1/FBγCyD** not only has the potential to serve as a basic structure of ATP chemosensing systems but also presents a desirable approach to exploit the concept of a **CyD**-based supramolecular chemosensor, which will be useful in various fields relating to molecular recognition. This presented concept holds promise to pioneer novel chemosensors for unexplored analytes.

Conflicts of interest

There are no conflicts to declare.

Acknowledgements

This work was financially supported by a JSPS Research Fellowship for Young Scientists PD Grant Number 21J00709 (Y.S.), and a JSPS Grant-in-Aid for Scientific Research Grant Number 20H02772 (T. Hayashita). We thank Ms Moeka Takahashi at Sophia University for her support regarding the synthesis of the probe.

References

1 D. Wu, A. C. Sedgwick, T. Gunnlaugsson, E. U. Akkaya, J. Yoon and T. D. James, *Chem. Soc. Rev.*, 2017, **46**, 7105–7123.
2 A. T. Aron, K. M. Ramos-Torres, J. A. Cotruvo Jr. and C. J. Chang, *Acc. Chem. Res.*, 2015, **48**, 2434–2442.
3 B. Huang, B. Liang, R. Zhang and D. Xing, *Coord. Chem. Rev.*, 2022, **452**, 214302.
4 M. Bonora, S. Patergnani, A. Rimessi, E. De Marchi, J. M. Suski, A. Bononi, C. Giorgi, S. Marchi, S. Missiroli, F. Poletti, M. R. Wieckowski and P. Pinton, *Purinergic Signalling*, 2012, **8**, 343–357.
5 I. Novak, *Physiology*, 2003, **18**, 12–17.
6 M. C. Jewett, M. L. Miller, Y. Chen and J. R. Swartz, *J. Bacteriol.*, 2009, **191**, 1083–1091.
7 A. R. Ribeiro, R. M. Santos, L. M. Rosário and M. H. Gil, *Luminescence*, 1998, **13**, 371–378.
8 D. de la Fuente-Herreruela, V. Gónzalez-Charro, V. G. Almendro-Vedia, M. Morán, M. Á. Martín, M. P. Lillo, P. Natale and I. López-Montero, *Biochim. Biophys. Acta, Bioenerg.*, 2017, **1858**, 999–1006.
9 Y. Zhou, Z. Xu and J. Yoon, *Chem. Soc. Rev.*, 2011, **40**, 2222–2235.
10 J. Krämer, R. Kang, L. M. Grimm, L. De Cola, P. Picchetti and F. Biedermann, *Chem. Rev.*, 2022, **122**, 3459–3636.
11 L. Wang, L. Yuan, X. Zeng, J. Peng, Y. Ni, J. C. Er, W. Xu, B. K. Agrawalla, D. Su, B. Kim and Y. T. Chang, *Angew. Chem., Int. Ed.*, 2016, **55**, 1773–1776.
12 Z. Xu, G. Zeng, Y. Liu, X. Zhang, J. Cheng, J. Zhang, Z. Ma, M. Miao, D. Zhang and Y. Wei, *Dyes Pigm.*, 2019, **163**, 559–563.
13 T. B. Ren, S. Y. Wen, L. Wang, P. Lu, B. Xiong, L. Yuan and X. B. Zhang, *Anal. Chem.*, 2020, **92**, 4681–4688.
14 Y. Rim Lee, N. Kwon, K. M. K. Swamy, G. Kim and J. Yoon, *Chem. – Asian J.*, 2022, **17**, 3–7.
15 H. T. Ngo, X. Liu and K. A. Jolliffe, *Chem. Soc. Rev.*, 2012, **41**, 4928–4965.
16 Y. W. Jun, S. Sarkar, K. H. Kim and K. H. Ahn, *ChemPhotoChem*, 2019, **3**, 214–219.
17 T. Minami, F. Emami, R. Nishiyabu, Y. Kubo and P. Anzenbacher Jr., *Chem. Commun.*, 2016, **52**, 7838–7841.
18 S. J. Butler and K. A. Jolliffe, *ChemPlusChem*, 2021, **86**, 59–70.
19 Y. Tsuchido, S. Fujiwara, T. Hashimoto and T. Hayashita, *Chem. Pharm. Bull.*, 2017, **65**, 318–325.
20 K. Aoki, R. Osako, J. Deng, T. Hayashita, T. Hashimoto and Y. Suzuki, *RSC Adv.*, 2020, **10**, 15299–15306.
21 K. Sugita, Y. Suzuki, Y. Tsuchido, S. Fujiwara, T. Hashimoto and T. Hayashita, *RSC Adv.*, 2022, **12**, 20259–20263.
22 S. Minagawa, S. Fujiwara, T. Hashimoto and T. Hayashita, *Int. J. Mol. Sci.*, 2021, **22**, 4683.
23 J. Yan, G. Springsteen, S. Deeter and B. Wang, *Tetrahedron*, 2004, **60**, 11205–11209.
24 G. R. Fulmer, A. J. M. Miller, N. H. Sherden, H. E. Gottlieb, A. Nudelman, B. M. Stoltz, J. E. Bercaw and K. I. Goldberg, *Organometallics*, 2010, **29**, 2176–2179.
25 ReactLab EQUILIBRIA, Jplus Consulting.
26 M. Levine and B. R. Smith, *J. Fluoresc.*, 2020, **30**, 1015–1023.
27 T. Yorozu, M. Hoshino and M. Imamura, *J. Phys. Chem.*, 1982, **86**, 4426–4429.
28 G. Bains, A. B. Patel and V. Narayanaswami, *Molecules*, 2011, **16**, 7909–7935.
29 T. Sakamoto, A. Ojida and I. Hamachi, *Chem. Commun.*, 2009, 141–152.
30 H. Shimizu, A. Kaito and M. Hatano, *Bull. Chem. Soc. Jpn.*, 1979, **52**, 2678–2684.
31 K. Fujita, S. Fujiwara, T. Yamada, Y. Tsuchido, T. Hashimoto and T. Hayashita, *J. Org. Chem.*, 2017, **82**, 976–981.
32 T. Yamada, S. Fujiwara, K. Fujita, Y. Tsuchido, T. Hashimoto and T. Hayashita, *Molecules*, 2018, **23**, 635.
33 C. Madry, I. L. Arancibia-Cárcamo, V. Kyrargyri, V. T. T. Chan, N. B. Hamilton and D. Attwell, *Proc. Natl. Acad. Sci. U. S. A.*, 2018, **115**, E1608–E1617.

